Preprint typeset in JINST style - HYPER VERSION

Using a CCD for the direct detection of electrons in a low energy space plasma spectrometer

Robert Bedington, Dhiren Kataria and Dave Walton

Mullard Space Science Laboratory - University College London
Holmbury St Mary, Dorking, UK

E-mail: robert.bedington@mssl.ucl.ac.uk

ABSTRACT: An E2V CCD64 back illuminated, ion implanted CCD (charge coupled device) has been used as a direct electron imaging detector with CATS (Conceptual And Tiny Spectrometer), a highly miniaturised prototype plasma analyser head. This is in place of an MCP (micro channel plate) with a position sensing anode which would more conventionally be used as a detector in traditional low energy space plasma analyser instruments. The small size of CATS however makes it well matched to the size of the CCD, and the ion implants reduce the depth of the CCD backside electron potential well making it more sensitive to lower energy electrons than standard untreated silicon.

Despite ionisation damage from prolonged exposure to excessively energetic electrons, the CCD has been able to detect electrons with energies above 500eV, at temperatures around room temperature. Using both a long integration 'current measuring' mode and a short integration 'electron counting' mode it has been used to image the low energy electrons exiting the analyser, enhancing our understanding of the CATS electrostatic optics.

The CCD has been proposed as the detector for use with CATS for an instrument on a low altitude student sounding rocket flight. Although it cannot detect the lowest energy electrons that an MCP can detect, and it is more sensitive to stray light, the low voltages required, the lack of vacuum requirements and its novelty and availability made it the most attractive candidate detector.

KEYWORDS: Particle detectors; Space instrumentation.

Contents

1. Introduction

Electrostatic plasma analysers are frequently used in space missions for the study of low energy (~ 0.1eV to ~ 40keV) space plasmas. They typically consist of a collimator, an electrostatic analyser head and a particle detector. Only plasma travelling on a limited range of trajectories can pass through the collimator to the electrostatic analyser. Of these particles only those within a limited range of kinetic energies can pass through the analyser head and onto the detector. The central energy and the range of energies of the particles that the analyser head lets through is proportional to the electric field in the analyser and thus is proportional to the voltage applied to the analyser electrodes.

The detector is typically a microchannel plate (MCP) with a position sensing anode or a channel electron multiplier (CEM). Although highly effective, these detectors require high voltages (kilovolts) and multiple channels of readout electronics.

With stringent mass and power constraints common in space applications MSSL (Mullard Space Science Laboratory) are currently developing prototype highly miniaturised, low resource plasma analysers [1] and are exploring alternative detector options. The small size of a typical CCD (charge coupled device) is well matched to the small sizes of our highly miniaturised analyser heads. Compared with MCPs, CCDs are easier to install and operate as they demand neither high voltages nor high vacuums, although they can require cooling systems which can present complications.

The miniature analyser head used in this experiment was CATS (Conceptual And Tiny Spectrometer). CATS is approximately 2x2x1cm in size and contains multiple channels of electrostatic optics to allow it to analyse multiple energies of electrons and multiple energies of ions simultaneously (up to approximately 8keV[1]) when a single voltage is applied to it. The energy selected

[1]This is for particles with a charge of $\pm 1e$ where e is the charge of an electron. In actuality the analyser is selecting by E/Q (energy to charge ratio), but since this paper deals only with electrons it is more convenient to refer to this as simply energy selection.

particles exit CATS out of tiny ($<0.4mm^2$) apertures, one for each channel, onto the CCD detector. Thus far it has only been tested with electrons.

While CCDs are more conventionally used to detect photons, their electron detecting capabilities have been well documented [2] [3]. When an ionising particle is incident on the CCD detector, it penetrates into the silicon and deposits energy in the form of electron hole pairs (transferring an average energy of 3.64eV per pair [4]) until it has lost all of its energy. The electrons in these electron hole pairs I refer to from here as 'generated electrons'. The generated electrons created are collected in the potential wells of the gate electrodes on the CCD front surface. It has been found that a standard front-side illuminated CCD makes a very poor electron detector, since firstly the gate structure interferes with the penetration of the electrons into the silicon and secondly irreversible damage is caused at the Si-SiO_2 interface [5]. Virtual phase CCDs alleviate some of these problems, for although they are front illuminated, they have electrodes that cover only half of each pixel, leaving the other half exposed. These CCDs have been shown to be effective detectors of electrons, although for incident energies under 10keV, they cannot compete with the detection efficiencies of back illuminated devices [3].

Back illuminated CCDs are those that have been removed from the substrate that they were built on and have had their undersides thinned. By this means the detection surface (the underside) is free of obscuring electrodes. At this exposed back surface a silicon-dioxide layer naturally grows and where this layer interfaces with the bulk silicon, positively charged defects are formed. The effect of these positive charges is to create a potential well for electrons at the CCD back surface. Any electrons produced in the vicinity of this region are attracted towards the backside rather than to the frontside electrodes and thus are not counted. This makes detecting low energy particles particularly problematic since their penetration depths into the CCD are very short. To mitigate this effect various treatments for the back surface have been devised [6]. The method that has been implemented on the CCD we are using here is ion implantation and laser annealing. In this method ions (e.g. boron) are forced into the back surface of the CCD where they create a field that reduces the depth of the backside well and raises the conduction band energy above that in the drift region. This raising of the conduction band causes a slope in the potential, which works to sweep secondary electrons created beyond the well towards the front of the CCD. The ion implanting process causes damage to the silicon lattice which if left unrepaired would result in high dark currents and low quantum efficiency. This is corrected by the laser annealing step mentioned above, which is able to reform the lattice.

An alternative CCD treatment, delta doping, reduces the depth of the back surface potential well even further, allowing an order of magnitude lower particle energies to be detected [7]. In this process molecular beam epitaxy (MBE) is used to add a very thin (1.5nm) layer of silicon onto the back surface of the CCD with an even thinner but very dense layer of boron dopant embedded within it, just a few atomic layers from the back surface [8]. The doping profile is then similar to a mathematical delta function and so the process is thus named. Delta doped CCDs are also the most suitable detectors for low energy ions (whose mass causes their penetration depths to be much shorter than electrons with the same energy). They have been found to be sensitive to incident protons down to a minimum detectable energy of about 1keV compared to approximately 10keV for an ion implanted device and approximately 100keV for untreated devices [9]. A delta doped CCD would be an ideal detector for CATS, but it was not something we had immediately available

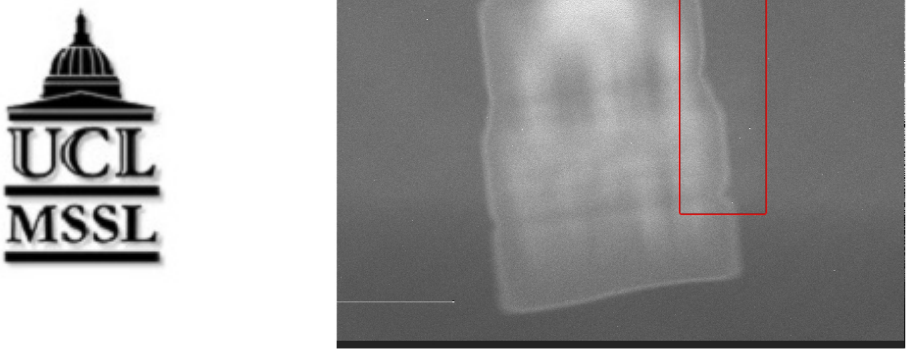

(a) The design used for the mask.

(b) The ionisation damage 'watermark' present in every CCD frame. The red rectangle marks the area directly below the CATS exit apertures.

Figure 1: Initial tests of the CCD with a laser cut mask and a nickel radioactive source caused permanent ionisation damage.

to us.

With our setup we have: imaged (for diagnostic purposes) the electron footprint from the CATS electrostatic optics; verified (in part) previous calibrations of the CATS response to electrons; performed initial investigations into using CCDs as detectors for low energy plasma analysers. Section 2 below discusses the experimental setup and the acquisition modes developed. Section 3 discusses briefly its use with the CATS analyser, the proposal to use this setup for an instrument on a sounding rocket and some of the detector trade-offs associated with that.

2. Detecting electrons with the CCD

We have used a back illuminated E2V CCD64-00 'x-ray' CCD sensor, a spare special-order CCD from the SXI instrument for the GOES programme [10], together with the engineering model readout electronics from the INTEGRAL-OMC instrument. The initial verifications of the electron detecting capabilities of the CCD were obtained using a nickel radioactive beta source. A laser cut copper mask (with the design shown in Figure 1a) was placed in front of the CCD and the beta source was placed in front of the mask. A fuzzy image of the mask confirmed that electrons were being detected. Interestingly, when the nickel source was removed some six to twelve days later and the CCD tested again, without the mask, there was still a fuzzy image of the mask in the centre of the frame with an intensity proportional to the integration time (see Figure 1b).

It appears to be permanent and has remained as a watermark on all raw images recorded since. The prolonged exposure to the energetic (up to ~65keV [11]) electrons from the nickel source caused ionisation damage and corresponding areas of increased dark current. This has increased

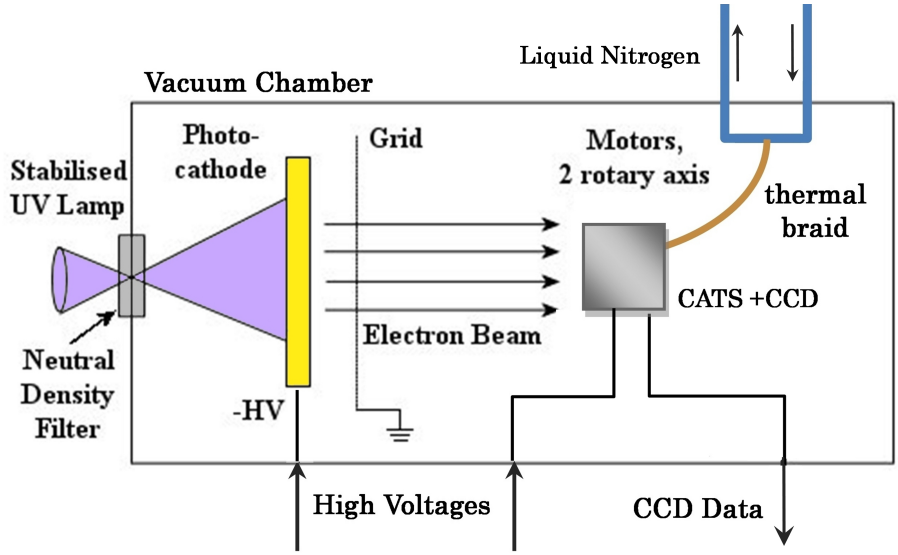

Figure 2: Schematic of the MSSL electron analyser calibration chamber.

the noise and halved the length of the integration times achievable before pixels become saturated with counts.

Subsequent tests used only electrons with energies of 2.5KeV and below which appear not to have caused any additional ionisation damage, although this has not yet been investigated thoroughly.

2.1 Experimental setup

The main tests were carried out in the MSSL electron analyser calibration facility using its flood electron gun, see figure 2. The UV lamp shines photons of an approximately fixed wavelength onto a photocathode. The photocathode is a quartz disc that is coated with a thin layer of gold/chromium that has a work function matched to the wavelength of the UV photons from the lamp. Accordingly when the lamp is shone on the coated disc photoelectrons with negligible kinetic energies are produced. A negative high voltage is applied to the metallic layer on the disc so that the photoelectrons are accelerated towards a fine electrically grounded grid in front of and parallel to the photocathode. Electrons that pass through the grid then drift towards the instrument under test as a monoenergetic flood beam, orthogonal to the photocathode and to the grid. The energy of the electron beam can be varied by changing the voltage on the photocathode and the intensity can be changed with neutral density filters. The instrument that is being tested is mounted at the centre of the beam on rotary stages with axes of rotation passing through this central point. Rotating the stage allows the beam to enter the instrument from different angles to allow a full angular calibration. While for studying the energy response of the CCD detector, the voltage on the photocathode can be varied to change the energy of the electrons, for studying the energy response of the CATS analyser head, it is preferable to use a fixed energy electron beam and to vary the voltage on the analyser electrodes. In this way the beam profile and detector response are constant. The calibration chamber setup is explained more extensively in [12].

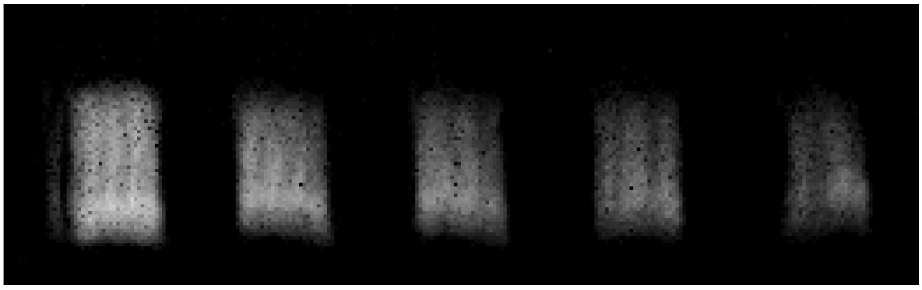

Figure 3: A composite image of the exit apertures of five CATS channels using the 'long integration, current detecting' method

Although the CCD dark current levels allowed for exposures of several seconds at room temperature, when the CCD was under vacuum it quickly heated up, increasing the dark current. A simple liquid nitrogen based cooling system was therefore set up which was able to take the CCD to just below room temperature for periods of several hours. It was a passive, unregulated system however, so the CCD temperature tended to vary by a few degrees or fractions of a degree throughout the tests.

2.2 Long integration acquisition mode

A simple and effective method for the CATS calibration and aperture imaging was to take images with as long an acquisition time as possible before pixel saturation occurred (several seconds). Figure 3 shows a composite of a few hundred, processed, long integration images showing electrons detected through some of the CATS channels during a voltage scan test performed at a few different angles. The area shown here is a smaller area within the red rectangle in Figure 1b. The five bright rectangles are the electron footprints from five of the CATS energy channels. They are 0.3mm wide and 0.4mm apart. The CCD pixels are 16μm squares, making each CATS aperture about 20 pixels across. The electrons detected here all have the same energy; the varying brightness between channels seen here is due to different throughput factors in the electrostatic optics. The banding seen within each of the aperture footprints is an effect of combining together images taken at several discrete voltage and angular steps.

The equivalent compilation of pre-processed, full-sized, raw image frames from which Figure 3 is obtained is in fact that shown previously in Figure 1b. To reveal the electron signal the image was processed thus: First a simple de-spiking algorithm (despike gen from the Solar Soft package)[2] was run on each raw image frame, removing hot pixels and electronics induced features. A similarly de-spiked background frame was then subtracted from each image frame to reveal just the electrons and any residual noise. The background frame is an exposure of the same integration time as the image frame, except with the analyser voltage reduced such that there were no electrons transmitted to the detector. As well as the thermal noise (mask shaped and otherwise) the background frame also included the large amount of stray UV light from the electron gun that was being reflected through the analyser head to the detector. In this acquisition mode a background frame would be taken as the first frame in a CATS voltage scan sequence each time the analyser was moved to a

[2] http://www.lmsal.com/solarsoft/

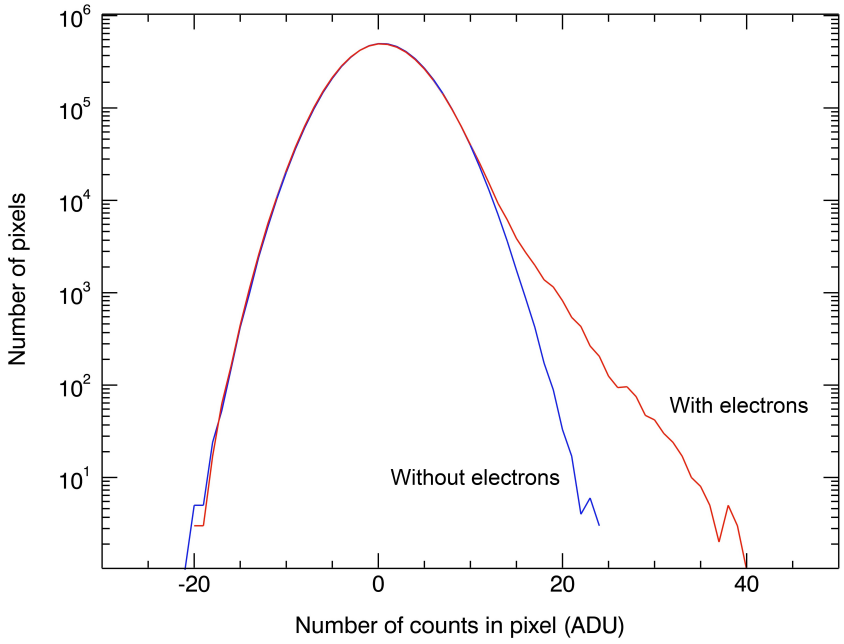

Figure 4: Histogram with logarithmic y axis of pixel values from many consecutive frames of 'background' subtracted short integration (particle mode) images. The blue line is for pixels under an inactive aperture and thus shows typical noise. The red line is the curve for pixels under an aperture transmitting 2.5keV electrons.

new angular position. It was found however that by the end of the voltage scan, there had usually been a noticeable change in the dark counts (i.e. temperature) and the background frame would no longer be representative of the true background counts in the image. To account for this the unused part of the CCD background image frame (i.e. everything outside of the aperture area) was scaled so its mean was the same as the corresponding area in the image frame. This means that a fraction of the reflected UV light (which is essentially independent of the detector and its temperature) is present in the final image. This effect appears to be negligible however.

2.3 Short integration acquisition mode

While the long acquisition method effectively measures a current of electrons, the second method aims to detect individual particles by using the shortest integration times the CCD electronics would stably allow, about 40ms. In this mode several hundreds of frames were taken consecutively and no specific background frames were recorded. In most frames there were a few (perhaps two or three) pixels that were clearly above the local noise profile and located almost exclusively in the aperture area. To extract only these events, the frames were de-spiked (to remove much larger electronics induced spikes) then summed and averaged. This averaged frame was then subtracted from each of the individual frames, again scaling for temperature variations in a similar way to that previously mentioned. With only a few electrons in each frame these would appear as small peaks above the residual noise after the subtraction.

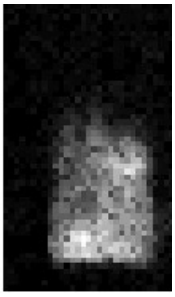

Figure 5: A 'short integration mode' image of 2.5keV electrons from a single CATS channel, consisting of ~1000 40ms frames taken at a single voltage and a single angular position.

Figure 4 shows a histogram of pixels values, from many thousands of these averaged-frame subtracted, short-integration frames. Pixel values from pixels in an area of the frame exposed to 2.5keV electrons are shown plotted as a red curve. Pixel values in an identically sized area of the frame with no electrons bombarding, are plotted as a blue curve. The blue curve counts are therefore solely attributable to noise sources; shot noise added by the electronics (read noise) is approximately 4 ADU (analogue digital units), effects associated with the averaging and scaling process used to generate the background frame will have some effect, but the largest contribution is from the shot noise on the dark current.

It can be seen that from above about 12 ADU there is a clear electron signal present in the red curve, but that any pixel cannot unambiguously be considered to be an electron unless it is greater than about 25 ADU. In the short integration data therefore, after the processing described above, any pixels below a threshold of 1.5 standard deviations of the pixel values of the non aperture areas (which corresponds to the point where the red and blue curves diverge) were zeroed. With increased cooling the dark current shot noise could be decreased, so the blue noise curve would be narrowed and the electron signal could be better resolved.

Figure 5 shows an image from data acquired in this mode. It shows 2.5keV electrons from a single CATS channel and consists of ~1000 40ms frames. Unlike Figure 3, this data has been acquired at a single CATS voltage and angular position. Some noise counts in dark shades of grey are just discernible in the background corresponding to the signal/noise overlap region previously discussed. This shorter integration, single particle method is of relevance to real space missions, where high sampling rates are required to resolve the time variation of particle fluxes and for spinning spacecraft to resolve the direction the particles have come from. The lack of a requirement of a background frame allows the instrument to be continuously detecting particles without gaps in the data.

2.4 CCD Energy Response

To study the response of the CCD to the energy of incident electrons, the energy of the electron beam was varied and the voltage on the CATS analyser adjusted accordingly so the profile of the beam on the detector remained constant.

The gain of the readout electronics is 1 ADU per 24 generated electrons. Correspondingly the long integration, 'current mode' acquisition method was able to detect the lowest energy electrons since generated electrons from multiple incident electrons could accumulate in a single pixel up

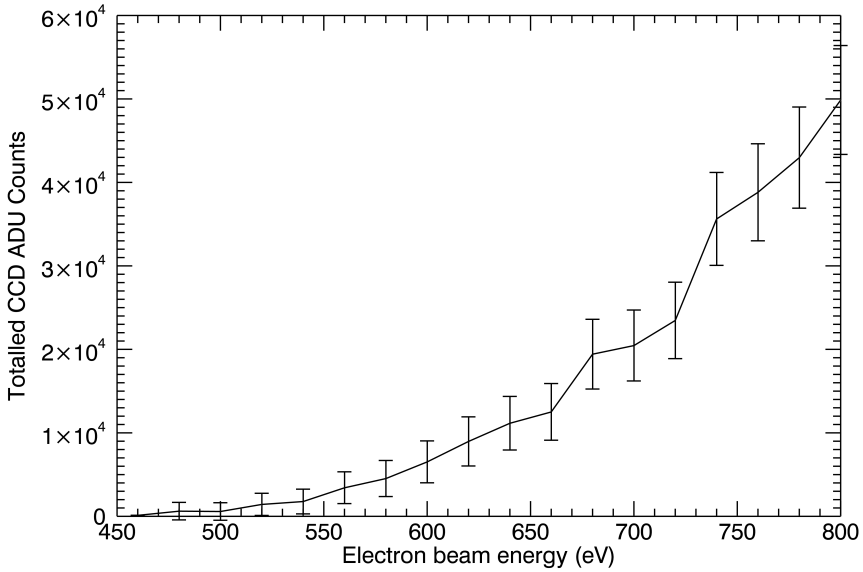

Figure 6: Total ADU counts in the aperture area over several images for different incident electron beam energies using the long integration method.

to a readable level (24 electrons). Figure 6 shows this variation in the total ADU counts over the aperture area for background subtracted, long integration images, summed over many image frames. It can be seen that the lowest energy electrons detectable are about 500eV and that at higher energies the signal generated by the electrons increases non linearly. This will be discussed in section 2.5. The length of the integration times for the lowest energy tests were limited by the time it took for pixels to become saturated by dark current counts. It is possible that with longer integration times lower energies of incident electrons could be detected with this method. This would require better cooling however or a CCD with less ionisation damage.

Using the short integration time, single particle method, the lowest energies detectable were about 800eV. Figure 7 shows how the incident electron energy affects the typical signal in a pixel of a fully processed image taken using this method. This figure has been obtained in the same way as Figure 4, but with the 1.5 standard deviation threshold applied (as discussed in section 2.3). It can be seen that higher energy incident electrons typically have higher pixel values, corresponding to more secondary electrons deposited and collected. As the beam energy is reduced, the electron signal disappears into the noise.

2.5 Simulation

To simulate the electron deposition within the CCD, a Mulassis [13] simulation was set up. Mulassis is GEANT4 based code produced by Qinetiq and freely available through the SPENVIS website[3]. While the necessary parameters for the CCD were largely unknown, such as the dead layer

[3] http://www.spenvis.oma.be/

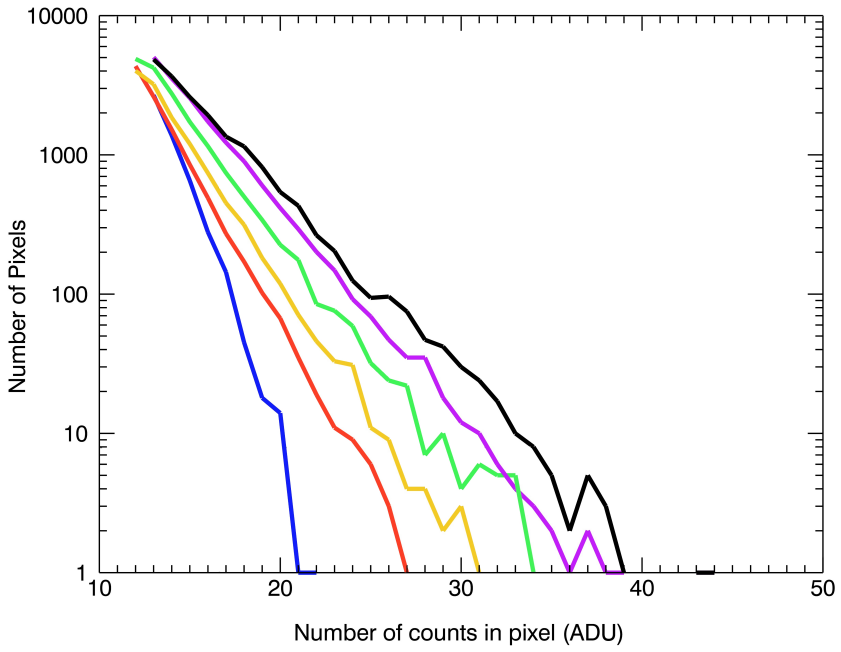

Figure 7: Histogram of pixels, from corrected short integration images, with the threshold cut-off applied, for electron beams of different energies. From left to right the curves correspond to; blue-no beam, then electron beam energies of; red-1.33keV, yellow-1.48keV, green-1.64keV, purple-1.82keV, black-2.25keV.

thickness, the ion implant depth and the initial charge collection efficiency (CCE)[4], we used numbers from [14] where a similar ion implanted CCD (a specially processed TekTronix TK512CB) is studied, so that at least a qualitative understanding could be gained. Figure 8 shows how the charge deposited by the penetrating electron varies with the energy of the electron and the depth of penetration. The charge collection efficiency is overplotted on this using two different semiempirical models, CCE1 as described in [14] and CCE2 as described in [3]. The CCE1 model has a dead layer where no charge is collected and a CCE that increases more gradually at first, whereas the CCE2 model assumes a small amount of charge is collected even at the back surface. The results they predict are similar however and it can be seen in the figure how the charge is deposited deeper in the CCD at higher energies. Only at 500eV (the dark blue curve) does the peak of the charge deposition occur beyond the dead layer. This is the lowest energy that we were able to measure electrons experimentally. By 800eV (the minimum energy at which individual electrons were experimentally detectable, using the short integration method) there is a much larger amount of charge being deposited beyond the dead layer (light blue curve) and significantly increased counts in the long integration method (as seen previously in Figure 6).

To investigate more directly the signal that would be produced in the CCD, the charge collected

[4]While in the bulk of the silicon all the charge deposited as generated electrons is collected by the electrodes (CCE=1), at the farthest distances from the front electrodes (i.e near the back surface) the CCE is significantly reduced.

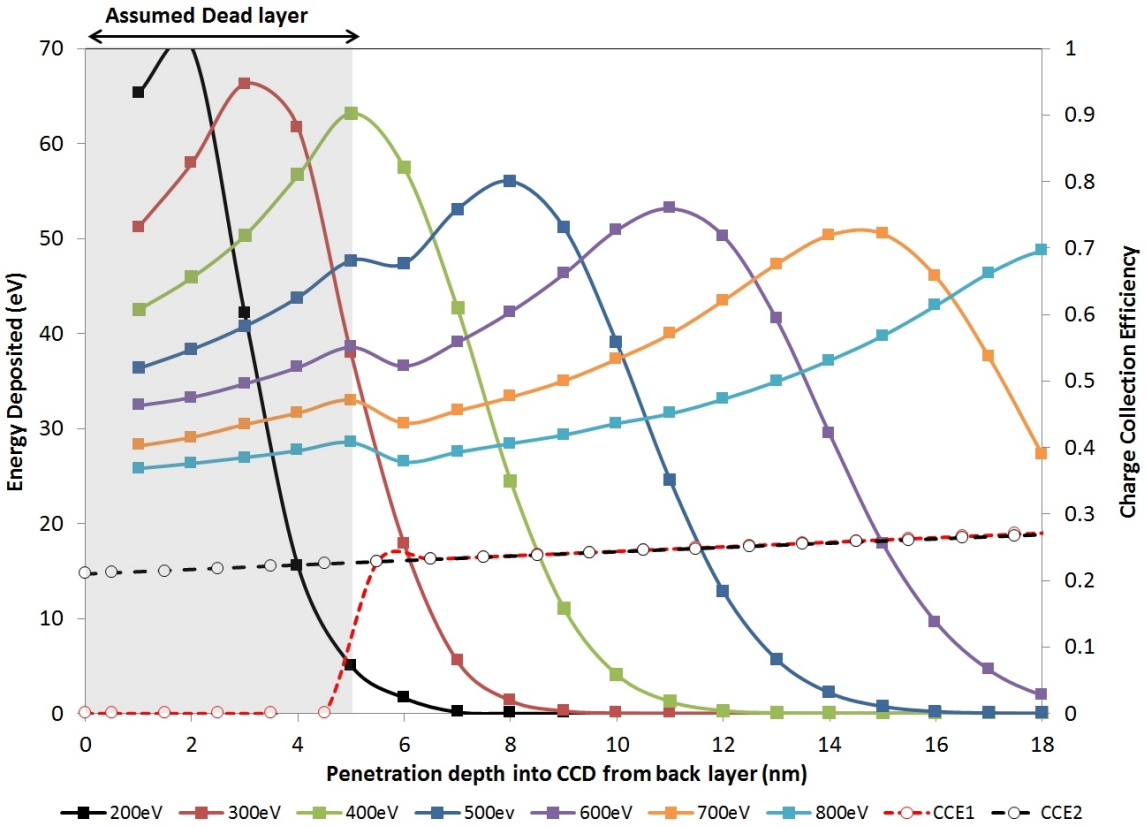

Figure 8: Mulassis simulated energy deposition of low energy electrons near the back surface of the CCD (assuming properties of Tektronix CCD in [14]). Also overlaid are the charge collection efficiencies, CCE1 and CCE2, calculated using two different methods.

was calculated at steps within the silicon by combining the charge deposited and the CCE that have just been described. The corresponding ADU signal per electron as a function of energy is plotted in Figure 9. It can be seen here how there is a non-linear region at low energies corresponding to where the charge collection efficiency is increasing. Once the electrons have enough energy to deposit their charge in the main bulk of the silicon where the CCE is unity, the eV to ADU relationship becomes linear. The energies we have been using in the experimental tests are shown in the inset box. Although the simulation has irregularities here, it is clear that the ADU values are less than 10, which would suggest that the peaks of the electron distributions in Figure 7 are buried in the noise.

3. A CCD detector for a low energy plasma spectrometer

The electron and UV footprint of the CATS channels has been imaged in many different positions, voltages and beam energies and this is enabling us to have a greater understanding of the subtleties of the electrostatic optics. Additionally, and as previously mentioned, the setup has been used to verify previous angular and voltage calibrations of the CATS analyser. These are achieved with computer control of the setup in Figure 2. Scripts are written to make CCD readings systematically

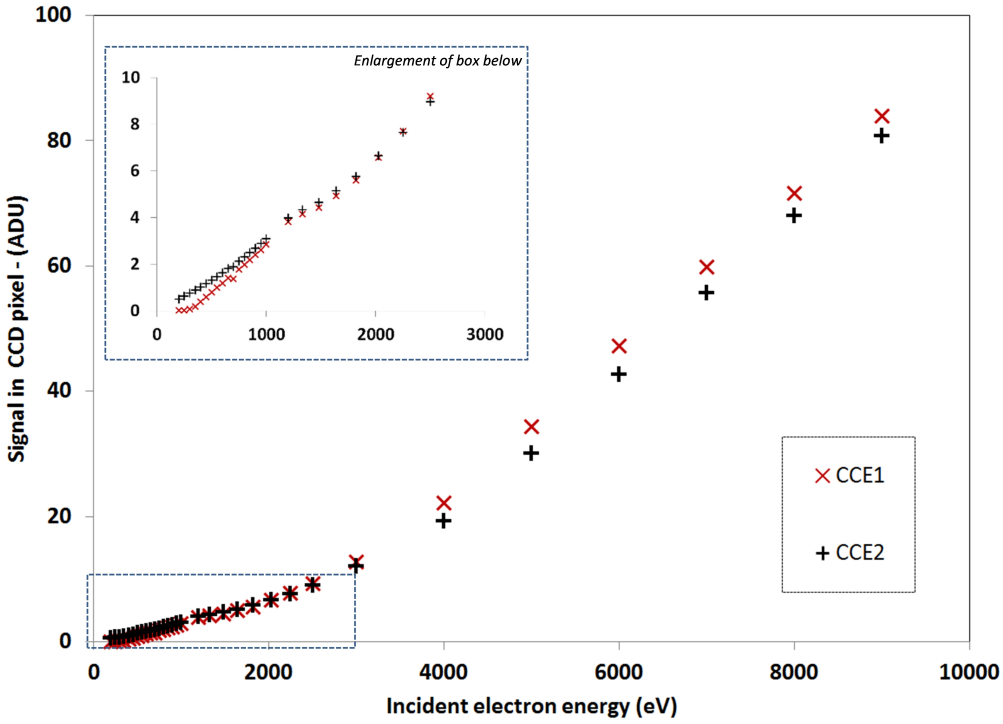

Figure 9: Simulated ADU counts per electron, for electrons of different energies, using data from Figure 8. The inset enlargement shows the region that has been investigated experimentally. Irregularities occur when the scale of the simulated Mulassis layers are changed as the higher energy electrons penetrate deeper into the silicon. CCE1 and CCE2 are two different methods for calculating the CCD charge collection efficiency.

over a range of analyser voltages or electron beam energies, for a range of different angular positions. The results are being used to verify previous calibrations made with a CEM detector in the same setup.

Figure 10 shows the response of the analyser to different electrode voltages (analogous to different beam energies). The separate peaks correspond to the different energy bandpass channels and their differing heights correspond to the different geometric factors of the channels (different throughput ratios). These data correspond directly with those in figure 3 .

With the concept demonstrated in the laboratory, the CATS analyser head and CCD detector combination have been entered as PoleCATS[5], a short-listed proposal for an instrument to study polar ionospheric and auroral electrons on REXUS 12/13 (Rocket-borne EXperiments for University Students)[6]. This is a payload opportunity on a low altitude sounding rocket to be launched from Esrange in Sweden in March 2013. Since funding is still being sought and likely to be extremely limited, the current component options are largely those that are available to us as donations. The CCD (using the short integration acquisition mode) is the detector selected to be used with CATS

[5] www.rexuspolecats.com

[6] www.rexusbexus.net

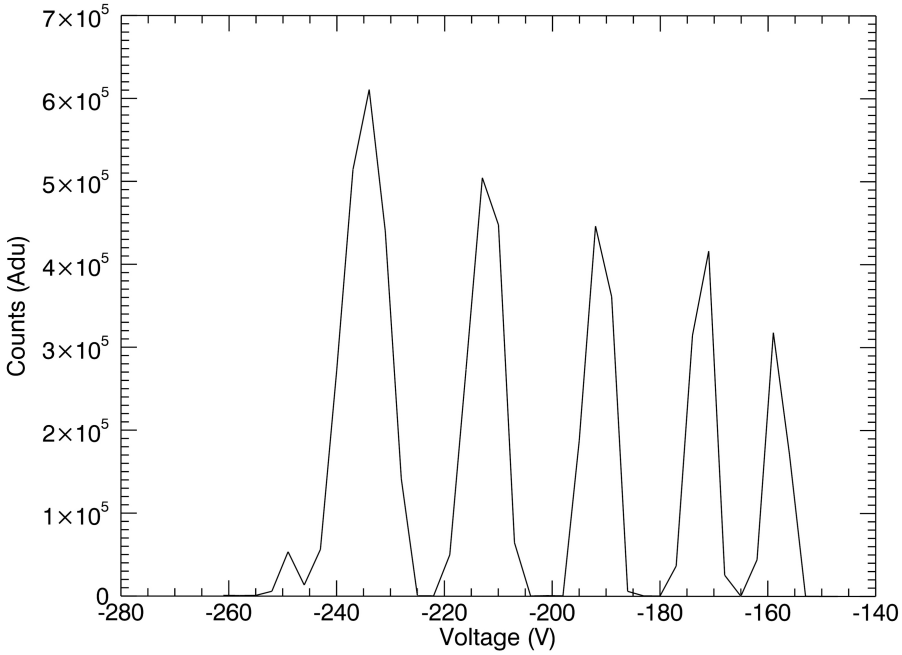

Figure 10: An example of a transmission response of five CATS channels at different analyser voltages to a 2.5keV monoenergetic electron beam. This is from the same data set is shown in Figure 3.

primarily because it is available and working and because it does not require high voltages and high vacuums. Its novelty as an electron detector also made it a more interesting candidate for what would essentially be a technology demonstration mission. The trade-offs that were considered for the detector choice are shown in Table 1 and are discussed below.

The direct electrode method, which would simply collect incident electrons on a collector plate electrode and measure their current directly (like in a Faraday cup instrument [15]) was ruled out as being insufficiently sensitive to the low fluxes of particles we expect to find. MCPs, which are usually the first choice of sensor for position-sensitive low-energy particle detectors, presented serious complications with respect to vacuum requirements. To prevent electrical arcing in an MCP, the tiny glass pores of which it is made must be free from air and moisture when it is in operation. To achieve this it needs to be under vacuum for a prolonged period of time to allow it to out-gas (dry out). For a satellite based instrument, which operates in the vacuum of space for long periods of time, this is easily accomplished. The REXUS rocket however is unlikely to be in atmosphere that is sufficiently thin with enough time for the MCP to out-gas and take measurements. To overcome this the MCP could be hermetically sealed and under vacuum prior to launch with a mechanism that releases a sealing door at the appropriate pressure/altitude, however this was deemed too complicated and risky for this instrument.

CEMS were the second choice of detector for the instrument. They have less strict vacuum requirements, are commonly used in low energy plasma instruments and have already been used with CATS. They could be operated in 'event mode' where they would perform like an MCP (only position insensitive), or in a current mode where they would operate similarly to the direct

electrode option but with electron multiplication. Although they are available in many sizes and configurations it is unlikely that we would find an affordable and workable solution that would allow us to use more than a couple of the CATS analyser channels since the channel exit apertures are very closely spaced, and one CEM would be needed to cover each aperture. Like MCPs, CEMs require kilovolts applied to them to work, which complicates the design of the power supply unit. The lack of this requirement from the CCD was another of its attractive qualities.[7]

The disadvantages to using the CCD, apart from its highly experimental nature, are that it is not sensitive to the lower energy electrons that MCPs and CEMs are able to detect. It is also very sensitive to photons, which the CATS analyser is not optimally configured to reject, and to temperature which will ideally be mitigated with cooling techniques. The cooling techniques in particular do add significant complexities. The data will also require significant processing. In the best scenario the instrument is successfully recovered and all the raw data is downloaded from flash memory for full processing on the ground. In case the memory is destroyed however, it is intended that some image processing would be performed on-board and down-linked to the groundstation, as it would be for a satellite mission. Since quality science data is not a high priority of the project, compared to education and technology demonstration, these disadvantages have been considered acceptable in view of the simplifications they enable and the novelty of the setup.

Acknowledgments

I would like to thank Alan Smith and Andrew Walsh for their suggestions, Reza Mirfayzi for his help with the CCD simulation work, and the STFC and EADS Astrium who have sponsored my PhD (RB). To find out more about PoleCATS and to get involved see www.rexuspolecats.com.

References

[1] R. Bedington, D. Kataria, A. Smith, S. Eckersley, *Development of a highly miniaturised low resource plasma analyser suitable for small satellite applications*, in Proceedings of *The 4S symposium (small satellites systems and services symposium)*, 31 May – 4 June, 2010 Funchal, Madeira

[2] T. Daud, J.R. Janesick, K. Evans, T. Elliott, *Charge-coupled device response to electron beam energies of less than 1 keV up to 20 keV*, *Opt. Eng.* **195** (1982) 323-325

[3] D.G. Stearns, J.D. Wieldwald, *Response of charge-coupled devices to direct electron bombardment*, *Rev. Sci. Instrum.* **60 (6)** (1989) 1095-1103

[4] J.R. Fiebiger, R.S. Muller., *Pair-Production Energies in Silicon and Germanium Bombarded with Low-Energy Electrons*, *J. Appl. Phys.* **43** (1972) 3202

[5] J.C. Cheng, G.R. Tripp, L.W. Coleman, *Intensified CCD readout system for ultrafast streak cameras*, *J. Appl. Phys.* **49** (1978) 5421

[6] J.R. Janesick, *Scientific charge-coupled devices*, SPIE Press, Bellingham, WA 2001

[7] S. Nikzad, Q. Yu, A.L. Smith, T.J. Jones, T.A. Tombrello, S.T. Elliott, *Direct detection and imaging of low-energy electrons with delta-doped charge-coupled devices*, *App. Phys. Lett.* **73** 3417 (1998)

[7] Although high voltages are still required for the CATS analyser head, these are still several times lower that those demanded by MCPs and CEMs.

[8] M.E. Hoenk, P.J. Grunthaner, F.J. Grunthaner, R.W. Terhune, M. Fattahi, H-F. Tseng, *Growth of a delta-doped silicon layer by molecular beam epitaxy on a charge-coupled device for reflection-limited ultraviolet quantum efficiency App. Phys. Lett.* **61** 1084 (1992)

[9] S.T. Lepri, S. Nikzad, T. Jones, J. Blacksberg, T.H. Zurbuchen, *Response of a delta-doped charge-coupled device to low energy protons and nitrogen ions*, *Rev. Sci. Instrum.* **77**, 053301 (2006)

[10] R.A. Stern et al., *Characterization of the flight CCD detectors for the GOES N and O solar x-ray imagers Proc. SPIE* 5171, **77** (2004)

[11] I.L. Preiss, R.W. Fink, B.L. Robinson, *The beta spectrum of carrier-free $Ni^{6}3$, J. Inorg. Nucl. Chem.* **4**, 233 (1957)

[12] G.R. Lewis et al., *The calibration of the Cassini Huygens CAPS Electron Spectrometer*, *Planetary Space Sci.* Vol. 58, No. 3 (2010) 427-436

[13] F. Lei, et al., *MULASSIS: a Geant4-based multilayered shielding simulation tool*, *IEEE Trans. on Nucl. Sci.*, **49**, 6, (2002) 2788

[14] R.A. Stern, L. Shing, M.M. Blouke, *Quantum Efficiency measurements and modeling of ion-implanted, laser-annealed charge-coupled devices: x-ray, extreme-ultraviolet, ultraviolet and optical data*, *Applied Optics* Vol. 33, No. 13 (1994) 2521

[15] H.S. Bridge, C. Dilworth, B. Rossi, F. Scherb, E.F. Lyon *An instrument for the investigation of interplanetary plasma*, *J. Geophys. Res.* **65 (10)** 2053 (1960)

Table 1: Trade-off table for a detector for the CATS plasma analyser on a proposed instrument for a REXUS sounding rocket

	Direct Electrode	**MCP**	**CEM (Current Mode)**	**CEM (Event Mode)**	**CCD**
Approx minimum detectable energy	1ev	1ev	1ev	1ev	1Kev (electrons only)
Simultaneous CATS channels usable	10	5 (either electrons or ions)	2-4 (insufficient space to fit 1 per channel)	2-4 (insufficient space to fit 1 per channel)	5 electrons (CATS ion energies too low to be detectable)
Number of incident particles required for data point	$6x10^6$ per pA	1	6 per pA	1	1
Vacuum Required	No	$1x10^{-6}$ mbar	$< 1x10^{-5}$ mbar	$1x10^{-5}$mbar	No, although cooling could cause condensation.
Outgassing issues	No	Yes, would need to be in vacuum from launch or a very large pore MCP (rare)	Fewer	Fewer	No
Read out electronics	Femto/pico ammeter per channel	Pre-amp + shaping amp + counter per channel	Nano ammeter (floating at high voltage	Pre-amp + shaping amp + counter per CEM	Clock controllers etc
Power supply	Low voltage	~2-3kV, 30μA	~1kV	~2-3kV, 30μA	32V